http://dx.doi.org/10.5935/0103-5053.20140111

J. Braz. Chem. Soc., Vol. 25, No. 8, 1317-1325, 2014.
Printed in Brazil - ©2014 Sociedade Brasileira de Química
0103 - 5053 $6.00+0.00

Article

Carbon-Supported PtSnCu, PtCu and PtSn Electrocatalysts for Ethanol Oxidation in Acid Media

Monah M. Magalhães and Flavio Colmati*

Laboratório de Eletroquímica (LabEl), Instituto de Química, Universidade Federal de Goiás, CP 131, 74001-970 Goiânia-GO, Brazil

Eletrocatalisadores de PtSnCu, PtSn, PtCu e Pt ancorados em carbono foram sintetizados através da redução química dos íons metálicos em solução por refluxo de etanol. Estes materiais foram caracterizados por espectrometria de raios X dispersiva em energia (EDX), difração de raios X (XRD) e microscopia eletrônica de transmissão de alta resolução (HRTEM) e eletroquimicamente por voltametria cíclica e cronoamperometria na presença e ausência de etanol no eletrólito. Todos os materiais mostraram uma distribuição homogênea no suporte de carbono com pouca formação de aglomerados. Os tamanhos de partículas ficaram em torno de 2-4 nm e foi observada a formação de solução sólida. A caracterização eletroquímica dos materiais mostrou estabilidade dos materiais e uma drástica diminuição no potencial de início de oxidação de etanol quando Cu modifica o catalisador de PtSn.

Carbon-supported PtSnCu, PtSn, PtCu and Pt electro-catalysts were prepared by reduction of metal precursors in ethanol reflux. These materials were characterized by energy-dispersive X-ray spectroscopy (EDX), X-ray diffraction (XRD) and high resolution transmission electron microscopy (HRTEM). Electrochemical properties were characterized by cyclic voltammetry and chronoamperometry in presence and absence of ethanol in the electrolyte solution. Results showed a metal nanoparticle homogeneous distribution on the carbon support with small agglomerate formation, particle sizes were determined as 2-4 nm and solid solutions formation were observed. The electrochemical characterization evidenced the material stability and a drastic decrease of the onset potential for ethanol electrochemical reaction was observed when Cu is used as a modifying compound to the PtSn electrocatalyst.

Keywords: PtSnCu, electrocatalysis, DEFC, ethanol oxidation, PEMFC

Introduction

Fuel cells convert chemical energy directly into electrical energy with high efficiency and are extremely attractive as power sources for application in mobile, stationary and portable devices.[1] Proton exchange membrane fuel cells (PEMFC) are supplied by the hydrogen molecule, which, at the anode, is split into proton ions and electrons and separate from each other, since protons permeate across the electrolyte to the cathode while the electrons flow through an external circuit, resulting in electric power. Also in the cathode, oxygen molecules from the air capture the free electrons, combine to the protons, resulting in water production. Moreover, PEMFCs operate at low temperature (70-100 °C), which is one of their major advantages.

*e-mail: colmati@ufg.br

However, since there are some issues on handling the hydrogen fuel, liquid fuels are thought to be more convenient for mobile applications and this is the reason why direct ethanol fuel cell (DEFC) have attracted the attention of the industries and of the scientific community. Among the major advantages of employing ethanol as fuel are its low toxicity, it is produced from agricultural row materials in large scale[2] despite low toxicity, it is preferred instead of methanol due to its higher theoretical mass energy density (8.01 kWh kg^{-1}), which is 1.3 times higher than that of methanol (6.09 kWh kg^{-1}).[3]

Although there are some similarities in the oxidation of low molecular weight alcohols when platinum (Pt) is employed as catalyst, because CO is produced as intermediate, better catalysts, which are more selective, have been studied. For example, in preliminary studies, Delime *et al.*[4] and Nonaka *et al.*[5] suggested the substitution

of Pt catalyst by Tin (Sn) and they found very interesting results leading to the oxidation of ethanol at lower potentials than those obtained when pure platinum is employed as catalyst.[6] In a previous work, the modification of Pt by copper prepared by formic acid method showed [7] that the catalyst were used to oxygen reduction reaction in a direct methanol fuel cell. Oezaslan *et al.*[8] showed PtCu alloy activity for oxygen reduction reaction in acid and alkaline media. On the other hand, Huang *et al.*[9] showed PtCu alloy with high density of surface Pt defects for ethanol oxidation. Lamy and co-workers[10-12] and Xin and co-workers[13-18] investigated the ethanol oxidation on carbon supported Pt-Sn catalysts prepared by distinct methods.[9,10] They showed that most of the Sn in the as-prepared catalysts was in a non-alloyed oxidized state and the use of these catalysts resulted in a remarkable enhancement of the observed current of direct ethanol fuel cells (DEFCs) with Pt-Sn as anode material. However, controversial results on the effect of the Sn content in the Pt-Sn catalysts on cell performance were reported. Lamy *et al.*[10] observed an optimum composition in which Sn is employed at the range of 10-20%, while Zhou *et al.*[15] found the optimum composition in the range of 33-40%, depending on the DEFC operation temperature. Also, Jiang *et al.*[16] compared the catalytic activity of a partially alloyed PtSn catalyst with that of a quasi-non-alloyed $PtSnO_x$ catalyst. They found that the slightly changed lattice parameter of Pt in the $PtSnO_x$ catalyst favors the ethanol adsorption and oxide formation in the vicinity of Pt nanoparticles conveniently provides oxygen species to remove the CO-like formed as ethanolic residues on Pt active sites. Colmati *et al.*[19] showed that PtSn obeys the Vegard's law when Sn content is varied in the catalyst, and although not all of the Sn content in catalysis was in the metallic form, there was oxide contents, both Sn forms contribute to ethanol oxidation, which leaded to the conclusion that Sn alloyed acts through electronic effects and Sn oxides act by bifunctional mechanism. On the other hand, when Pt catalyst is modified by Cu addition, the interaction between Pt and Cu that results in a slight oxide presence PtCu, which also obeys the Vegard´s law, when Cu content are varied in the catalyst. Oezaslan *et al.*[8] used the Vegard´s law to determine the compostition of the PtCu electrocatalysts for different Cu contents. Pt modified by Cu results in contractions of the lattice parameter, for PtCu (1:1) Oezaslan *et al.*[8] found 0.3808 nm, Carbonio *et al.*[7] found a lattice parameter of the $Pt_{70}Cu_{30}$ 0.391 nm and, in this work, was reported a lattice parameter of the PtCu of 0.3878 nm. In all samples, the lattice parameter of the PtCu is smaller than Pt (i.e., 0.3913 nm) which suggests the Cu insertion on the Pt lattice. Some differences are observed when these data are compared to those reported by Oezaslan *et al.*[8] but these seem to be due only to minor experimental errors or to equipment distinct sensitivities and should not be taken into account. In these compounds, it can be considered that all the amount of Cu added to the catalyst is inserted into the Pt lattice and part of amount of the Sn forms a superlattice in the catalyst, which is the reason for the observed good stability. Page *et al.*[20] had already developed a PtCu catalyst for methanol oxidation purposes and they observed that although severe surface Cu dissolution results in current oscillation,[20] PtCu also increases methanol activity. Also, Yang *et al.*[21] showed that PtCu nanoparticles are efficient in to the methanol oxidation and Carbonio *et al.*[7] reported their results on PtCu modified by Pd as a cathode of the PEMFC, revealing a improvement in the catalytic activity. It is also expected that the use of Sn as modifying agent on PtCu lattice can improve the activity of the final catalyst in the ethanol oxidation process.

In this way, several researchers have focused their studies on the trimetallic material to electro-oxidize ethanol, for example. Beyhan *et al.*[22] studied the influence of metals such Ni, Rh, Pt and Co as modifying agents in the PtSn electrocatalyst for ethanol oxidation and, they observed CO formation increase when trimetallic electrocatalysts are employed. Ribeiro *et al.*[23] investigated the influence of the Ir in the Ir-modified PtSn catalyst and observed that the onset potential of ethanol oxidation is less positive than that of PtSn. Recently, Silva-Junior *et al.*[24] synthesized PtRhSn and PtRh for ethanol oxidation and they observed higher ethanol oxidation current on trimetallic material, moreover, they found that this material is capable of converting ethanol to CO_2 when the Rh content in the catalyst is low. De Souza *et al.*[25] obtained PtSn modified by Ce, which resulted in an increase of the ethanol oxidation current. Silva *et al.*[26] prepared IrPtSn with low Pt content in the catalyst and, once again, the trimetallic material resulted in the increase of the electrochemical ethanol oxidation current, compared to that of PtSn from E-TEK. These are a few examples that the multi-metallic catalysts should cleave the C-C bond of the ethanol molecule to achieve total conversion at low over potential.

In this work, carbon supported Pt-Sn, PtCu and PtSnCu alloy catalysts were prepared by reduction of Pt and Sn precursors at ethanol reflux. The final products were characterized by X-ray diffraction (XRD), high resolution transmission electron microscopy (HRTEM) and their electrocatalytic activities for ethanol oxidation were compared to those of commercial Pt/C electrocatalysts from E-TEK.

Experimental

Catalyst preparation

The electro-catalysts were prepared by chemical reduction of the starting metallic ions in solution and in ethanol reflux for 3h. The obtained materials were filtered, washed and dried by a procedure similar to that related by Spinacé *et al*.,[27] which could be considered as a polyol method adaptation.[28] For this procedure, an appropriated mass of carbon powder (Cabot Vulcan XC72R) was suspended in 1 mol L^{-1} ethanol aqueous solution. Solutions of the $H_2PtCl_6.6H_2O$ (Sigma-Aldrich), $SnCl_2.2H_2O$ (Vetec) and $CuCl_2.H_2O$ (Vetec) freshly prepared were added to the carbon suspension, which was heated to boil and refluxed for 3 h. Afterwards, the suspension was left to cool at room temperature and the solid filtered and dried in an oven at 60 °C for 1 h. The materials were 20% (w/w) metal on carbon.

Energy dispersive X-ray analysis (EDX)

The atomic ratios of the PtM_1M_2/C catalyst were determined by the energy dispersive X-ray analysis technique coupled to a scanning electron microscope, Jeol, JEM-2100, Thermo scientific.

X-ray diffraction (XRD)

The materials were morphologically characterized by XRD in a Shimadzu XRD-6000 diffractometer, the scan rate was a step at 0.02° s^{-1} between 20 and 100 degree in 2θ. For this purpose a part of the catalyst was deposited at sample hold and placed into diffractometer.

High resolution transmission electron microscopy (HRTEM)

The samples for the high resolution transmission electron microscopy characterization were prepared as follows: a carbon film was deposited onto mica sheet that as placed onto the Cu grids (400 mesh and 3 mm diameter). The material to be examined was dispersed in water by sonication, placed onto the carbon film, and left to dry.

Histograms of particle sizes were constructed using about 300 particles. This technique was implemented in the Microscopy Laboratory of the Laboratório de Microscipia Multiusuários da Universidade Federal de Goiás (LABMIC) using a HRTEM microscope JEOL, JEM 2100, URP, operating at 200 kV and having a resolution of 0.2 nm.

Electrochemical measurements

For electrochemical experiments the catalysts were ultrasonically dispersed in water with isopropyl alcohol and a part of this suspension were deposited on previously polished glass-carbon with a diamond past (1 μm) and imbibed in a Teflon rod. Finally, the electrode was loaded with 100 μg of Pt. The electrode was inserted onto glass electrochemical cell with three electrodes, Pt gauze as auxiliary electrode, Ag/AgCl as reference electrode and the sample in the working electrode. The experiments were carried out in a 0.5 mol L^{-1} sulfuric acid medium and at distinct ethanol concentrations. The catalysts were characterized by cyclic voltammeter, linear sweep voltammeter and chronoamperomenter. All the experiments were carried out at room temperature.

Results and Discussion

The catalysts were characterized by EDX analysis, the real composition is shown in Table 1. It is noteworthy that the obtained materials atomic ratios are very close to the nominal composition.

Table 1. Results obtained from EDX analyses

Material	Real composition / %	Nominal composition / %
PtSnCu/C	36.52:37.49:25.99	33.33:33.33:33.33
PtCu/C	75.69:24.31	75.00:25.00
PtSn/C	69.64:30.36	75.00:25.00
Pt/C	100	100

X-ray diffraction pattern is shown in Figure 1. Peaks related to face cubic centered (fcc) structures, typical of Pt, are observed. The peak at 2θ = 25° is related to the carbon support, the peaks at 2θ = 40°, 47°, 67°, 82°, and 87° are associated to the (111), (200), (220), (311) and, (222) planes, respectively. The observed shifts on peak positions at larger angles can be attributed to insertion of the metals in the Pt lattice crystalline.

The lattice parameters of the material are shown in Table 2. The changes in the lattice parameter suggest the formation of the solid solution of Pt and Cu, whereas Sn is kept in its oxide form. The XRD results provided the same peak position shifts pattern as demonstrated in earlier works[7,18] in which PtSnCu presented shift peak positions to larger degrees with respect to Pt, whereas the peak of the PtSn shifts to lower degrees. Moreover, XRD showed peaks at 2θ = 37° and 2θ = 52° degrees, which are characteristics of the cassiterite (tin-oxide), marked by * in the Figure 1. The seven more important peaks which are characteristic

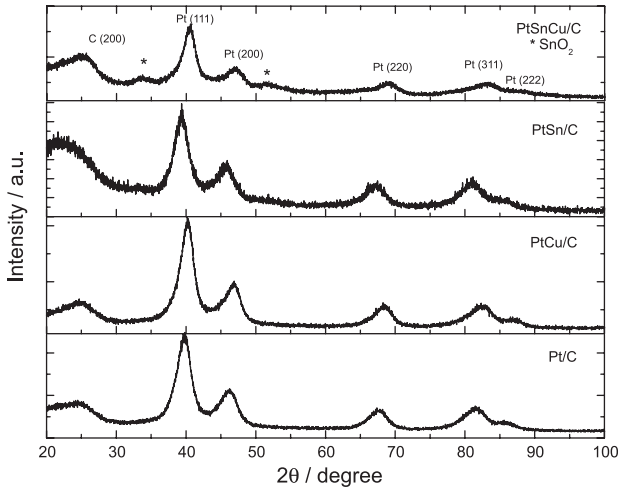

Figure 1. XRD patterns of the carbon supported 20 wt % PtSnCu, PtSn, PtCu and Pt catalysts.

of Cu/C[29] occur at ca. 36°, 38°, 42°, 43°, 50°, 61°, and 74°. The peaks located at 43°, 50° and 7 ° correspond to the fcc of Cu. The other peaks are related to presence of Cu oxides, more specifically CuO (36°, 38°) and Cu_2O (42°, 61°), neither one of these peaks were observed in XRD, nevertheless their presence cannot be disregarded, since they can be present even at small intensities or may be hidden.

Table 2. Cristal size and lattice parameter of the prepared electro-catalysts

Material	Crystal size / nm	Lattice parameter / nm
PtSnCu/C (1:1:1)	2.32	0.3859
PtSn/C (3:1)	2.11	0.3934
PtCu/C (3:1)	2.64	0.3878
Pt/C	2.70	0.3911
Pt/C-ETEK	2.85	0.3922

The crystal sizes were determined using the Scherrer equation,[23] for this purpose a peak 220 at 2θ = 65° degree was used. Although it is not the more intense peak, it is located at a position far enough from the 002 peak of the carbon and has a small background influence. The crystal sizes are around 2-3 nm and are shown in Table 2.

Figures 2a-d, present the results of the HRTEM analysis of the carbon supported PtSnCu, PtCu, PtSn and Pt catalysts prepared by the reflux of ethanol. HRTEM micrographs were obtained with magnifications of 200,000 fold. Images showed that the distribution of the metal particles on the carbon support is uniform and have a narrow particle size distribution. The particle size distribution histograms (Figures 3a-d), which include analyses of several different regions, quantitatively reflect the uniform size distribution of the catalysts. The mean particle diameter, d, was calculated by:

$$d_i = \sum_i \frac{n_i d_i}{n} \quad (1)$$

Where n_i is the frequency of occurrence of particle with size d_i. The material calculated mean particle size around 2-3 nm, which is in good agreement with crystal size obtained by XRD data. The average particle size for all the prepared catalysts are shown in Table 3. The Pt/C synthesized by ethanol reflux showed particle size similar to the Pt/C form E-TEK material reported in the literature.[30] The histograms of the particle size distribution, Figures 3a-d, which were obtained at several different regions, quantitatively reflect a Lorentz size distribution, except to PtCu , which reflects a Gauss size distribution.

Table 3. Particle size from TEM analysis

Material	Particle size / nm
PtSnCu/C (1:1:1)	3.0
PtSn/C (3:1)	3.3
PtCu/C (3:1)	2.5
Pt/C	2.9

Typical cyclic voltammograms of the catalysts in acid media are shown in Figure 4. Voltammograms were normalized by Pt load. All the materials showed the hydrogen adsorption/desorption regions with the peak associated to different crystalline faces exposed to the electrolyte, which are between −0.2 and +0.1 V *vs*. Ag/AgCl, larger, +0.1 to +0.8 V *vs*. Ag/AgCl, and also presented the double layer and oxides region that cannot be distinguished. The double layer capacitance grows despite the oxide presence in the same way to the ternary material, which posses tin oxides. Also, PtSn, which does not present a high alloy degree, showed an increase in a double layer capacitance. On the other hand, both results differ from what it had been observed for PtCu material, where the double layer capacitance was similar to Pt. It can be explained by the interaction between Pt and Cu that results in a slight oxide presence. Page *et al*.[20] had already studied PtCu for methanol oxidation and found the increase on methanol activity. Yang *et al*.[21] showed that PtCu nanoparticles were suitable to oxidation of methanol and, in this work, Cu and Sn were incorporated in Pt lattice and the XRD results suggest superlattice formation. It is possible once SnCu is an established alloy known as Ore. There are many distinct Ore compositions and, typically, it only oxidizes superficially; once copper oxide (eventually

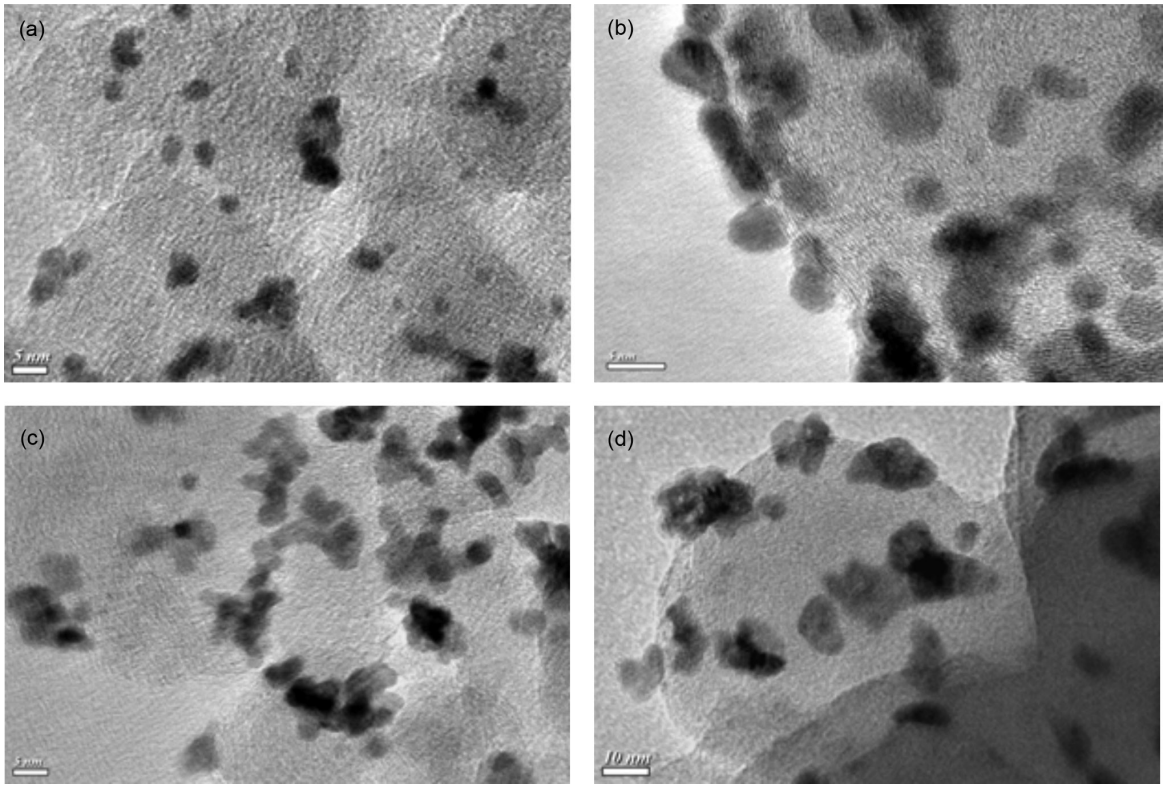

Figure 2. TEM images obtained for: (a) Pt/C; (b) PtSn/C; (c) PtCu/C and (d) PtSnCu/C.

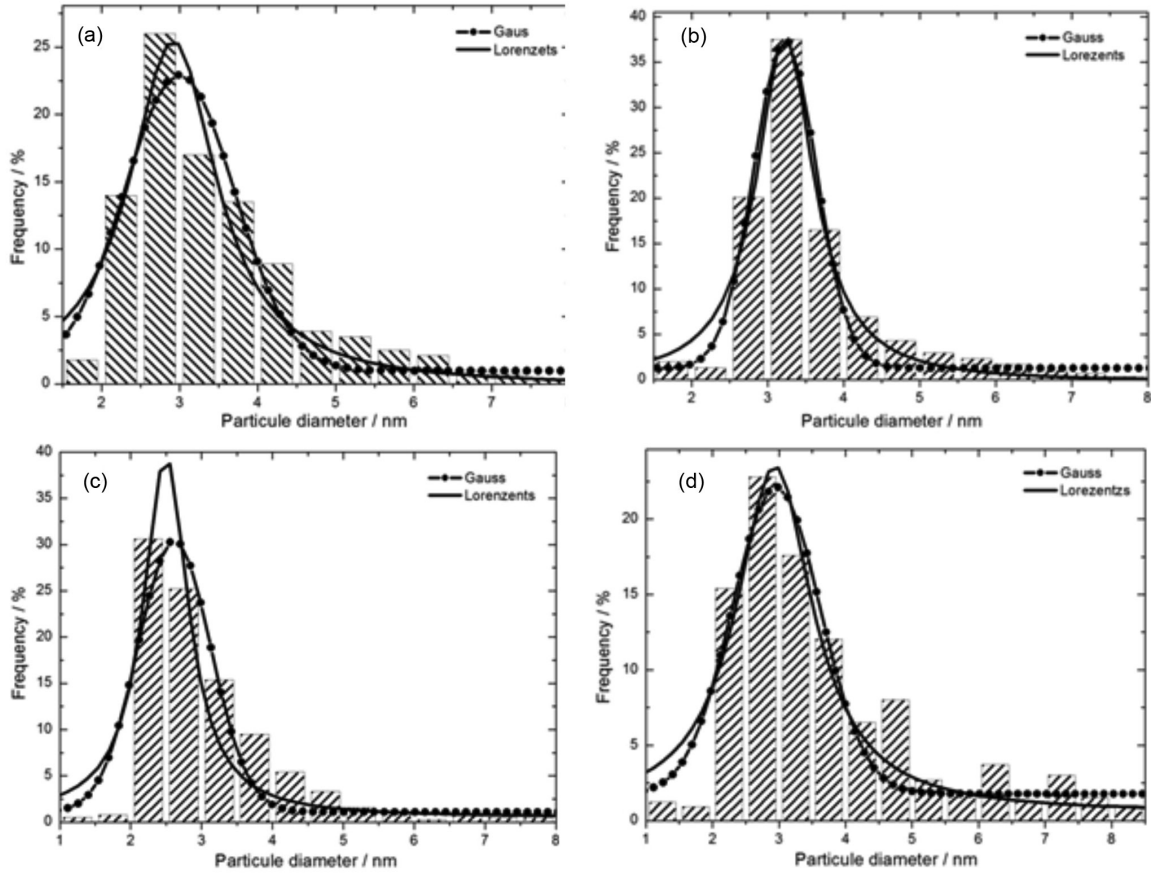

Figure 3. Histograms with the corresponding particle size distributions for: (a) Pt/C; (b) PtSn/C; (c) PtCu/C and (d) PtSnCu/C.

becoming copper carbonate) layer is formed, the underlying metal is protected from further corrosion. In the same way, Amman *et al.*[31] observed a superficially Cu dissolution but not Cu presence into the material bulk. Moreover, Cu have very good affinity with Pt, and in previews works it was related to Pt and Sn interaction.[32,33] Thus, the ternary materials can show thermodynamic stability.

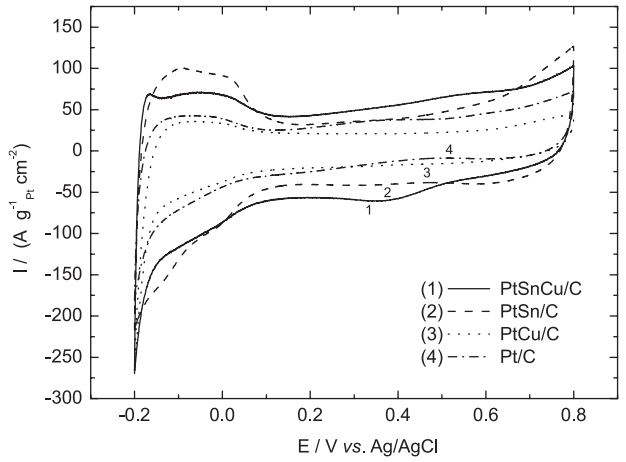

Figure 4. Cyclic voltammetry of PtSnCu, PtSn, PtCu and Pt in 0.5 mol L^{-1} sulfuric acid, scan rate of 50 mV s^{-1}, T = 25 °C.

Huang *et al.*[34] observed Cu behaviors in nanobelt electrode by cyclic voltammeter in a phosphate buffer solution (pH = 7.4), they found oxidation peaks at –0.02 V, 0.18 V and 0.32 V *vs.* Ag/AgCl, that were associated to the conversion of the Cu(0)/Cu+, Cu(I)/Cu(II) and Cu(II)/Cu(III) respectively, although in this word, the cyclic voltammeter were registered in acid media, these peaks were not observe. That suggests that the Cu content in the catalyst has not been oxidized, in other words, the Cu content in the catalysts prepared, containing PtSnCu and PtCu, has shown to be stable.

Figure 5 shows cyclic voltammeter of the catalytic material in presence of the 1 mol L^{-1} ethanol. In all cyclic voltammogram the electrochemical acidity for ethanol oxidation is observed and the onset potentials of the electrochemical are shown in Table 4, the onset potentials were considered as the potential value when the slope of the voltammograms exceeded 0.005 mA cm^{-2} mV^{-1}. It is noteworthy that the presence of the Cu and Sn drastically reduces the onset potential, as observed by cyclic voltammetry; the presence of these metals results in beneficial to ethanol oxidation process and their intermediates at lower potentials. Assuming that Cu and some Sn are in the alloy form, which is corroborated by the XRD peak position and presence of cassiterite, the observed decrease in the ethanol onset potential can be explained in terms of the two basic mechanisms previously described: electronic effect and bifunctional mechanism. In the former, the electronic interactions between Pt and Cu induce a modification in the ethanol adsorption energy. SnO_2 is well known for participating in strong platinum interactions, and indeed, this effect had been reported.[35] The origin of these interactions lies in the oxygen vacancies present in the amorphous surface oxide.[20,36] These vacancies may be able to trap electrons donated by Pt, which, in turn, would result in a weakening of the CO adsorption strength, facilitating its oxidation. The bifunctional mechanism is based on the donation of ^{-}OH species to Pt sites from neighbouring reducible oxide species at lower potentials than those required for Pt oxidation. The combination of these two mechanisms results in a decrease of the ethanol oxidation onset potential to –0.1 V *vs.* Ag/AgCl (this value was considered when the slope of the voltammograms exceeded 0.005 mA cm^{-2} mV^{-1}). Barroso *et al.*[37] obtained a PtSnCu electrocatalyst in amorphous alloys and observed an increase in the ethanol oxidation current compared to those of PtRuCu and PtSnRu, on the other hand, the onset potentials were above 0.4 V *vs.* Ag/AgCl, they attributed the higher oxidation current of PtSnCu to the electronic irregular configuration of the Cu ($3d^{10}$ $4s^{1}$) beyond that the Sn-oxides confer a special behavior to PtSnCu. In this work, a special behavior was observed for crystalline (fcc structure) PtSnCu on the ethanol electroxidation: the onset potential decrease, as presented in Figure 5.

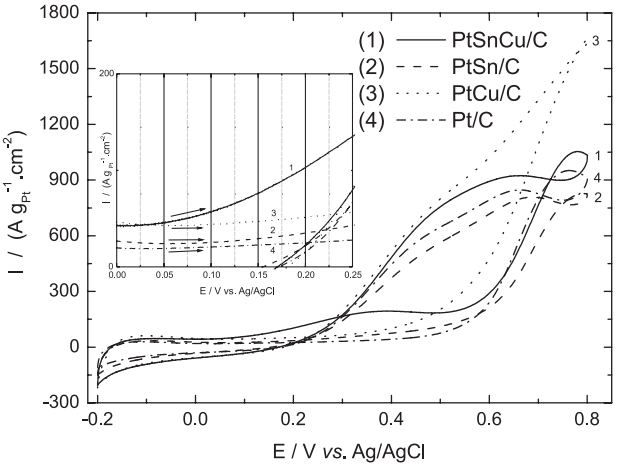

Figure 5. Cyclic voltammetric curves of PtSnCu, PtSn, PtCu and Pt in 0.5 mol L^{-1} sulfuric acid with 1 mol L^{-1} of ethanol solution, scan rate of 50 mV s^{-1}, T = 25 °C. Inset: enlarged view of the onset potential.

The performance of the PtSnCu PtCu, PtSn and Pt catalysts towards ethanol oxidation was also observed by chronoamperometry registered at 0.25 V *vs.* Ag/AgCl, data are shown in Figure 6. In all curves there is an initial current drop where PtSnCu display a superior performance. Then, PtSnCu/C kept showing a slower decay compared to PtCu/C

Table 4. Onset potential obtained from Figure 5

Material	Onset potential / V
PtSnCu/C	0.10
PtSn/C	0.27
PtCu/C	0.33
Pt/C	0.44

and PtSn/C and its current intensities become higher than those recorded after about 1800 s. Crisafulli *et al.*[38] reported their results for $Pt_{50}Sn_{30}Cu_{20}/C$ as electrocatalyst for ethanol oxidation and they observed a better performance for ternary material when compared with PtSn, they showed a considerable increase on electrochemical activity after acid treatment on catalysts. It demonstrates the relative stability of PtSnCu/C compared to other materials in the sulfuric acid media containing ethanol, the current of the ethanol oxidation obtained by PtSnCu are very similar to that registered for materials obtained by Crisafulli *et al.*[38] after acid treatment on catalyst.

The electrocatalysts stability were evaluated under cycled conditions, for this purpose, the chronoamperometry were registered before and after one hundred cycles voltammeter. The cyclic voltammograms are shown in Figure 7a. From Figure 7b, it can be inferred that the PtSnCu electro-catalysts loses 20% of current density at 1800 s, after 100 cycles, which characterizes the good stability of this materials. Zhang *et al.*[39] proposed that electrocatalysts degradation can be attributed to tree situations like that: *i*) particle agglomeration, *ii*) Pt loss and redistribution and *iii*) poisonous effects. The main less activity in this work could be attributed to poisonous effect because the electrode were cycled only 100 times.

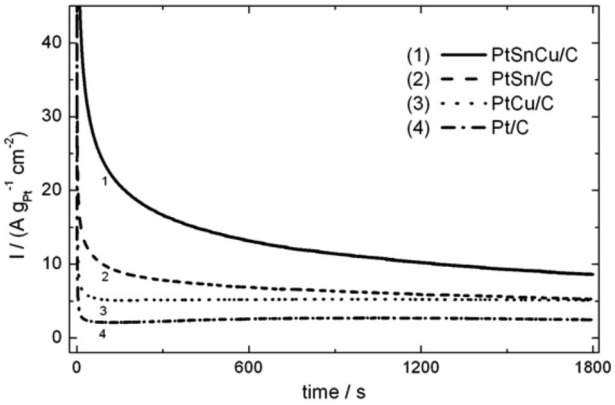

Figure 6. Chronoamperometry of PtSnCu, PtSn, PtCu and Pt in 0.5 mol L^{-1} sulfuric acid with 1 mol L^{-1} of ethanol solution, E = 0.25 V *vs.* Ag/AgCl, T = 25 °C.

Furthermore, the chronoamperometry registered before and after the cycles were registered in the same ethanol solution, namely, there are ethanolic residues in solution that poison the electrocatalyst. Ammam *et al.*[30] showed a similar stability study for quaternary metallic material and observed a similar current decrease, after 400 cycles. They observed a slight increase in the hydrogen adsorption region after 200 cycles that were attributed to a slight corrosion of the catalysts after cycling in sulfuric acid, thereat, with ethanol in electrolyte, they observed a current decrease after 200 cycles.

Conclusions

The EDX analysis showed to be an accurate methodology for electro-catalytic nanoparticle atomic ratio determination, as ratios close to nominal were obtained. Also, nanoparticles were assumed to present a homogeneous size distribution on carbon support, which was close to 3 nm.

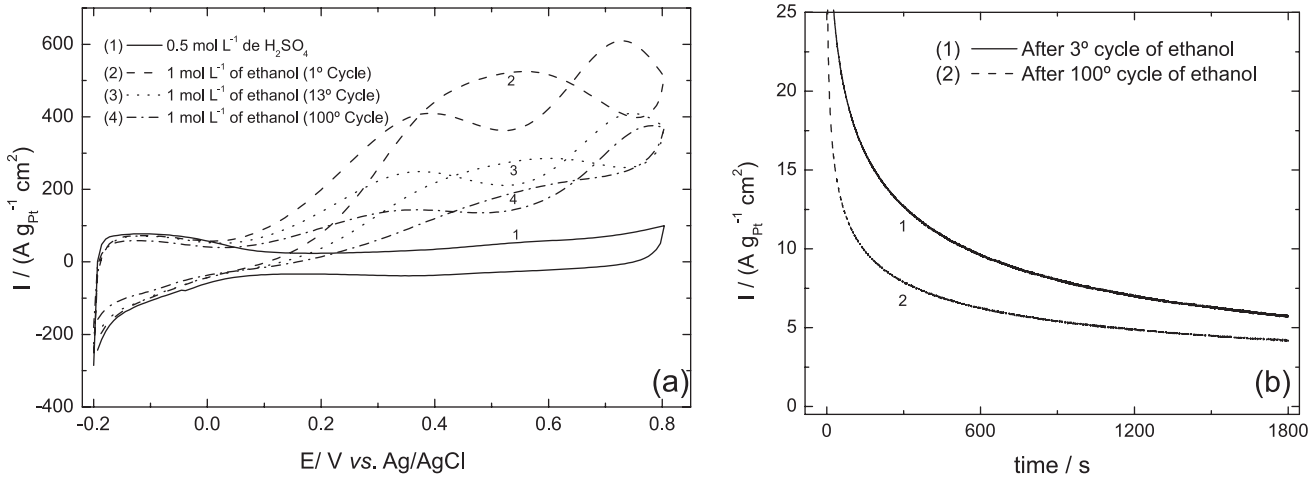

Figure 7. (a) Cyclic voltammetry PtSnCu/C in 0.5 mol L^{-1} sulfuric acid with 1 mol L^{-1} of ethanol solution, v = 50 mV s^{-1}, T = 25 °C; (b) chronoamperometry before and after 100 cycles of PtSnCu/C in fixed potential of 0.15 V, T = 25 °C.

The materials show a fcc structure and the Sn and Cu were proven to be inserted in the Pt lattice. The same for tin oxide was observed by XRD experiments.

All the catalysts prepared showed electrochemical activities for ethanol electro-oxidation in solution. Ternary material PtSnCu showed a drastic reduction of the onset potential in comparison with PtSn and PtCu beyond Pt. All materials showed a stable current at 1800 s.

The electrochemical stability of the PtSnCu material was evaluated under 100 cycles condition and a current decrease in cyclic experiment was observed, although it did not lead to a relevant change in the onset potential. From chronoamperometric experiments, the ethanol eletro-oxidation current on PtSnCu showed a small current decrease (at t = 1800 s).

Acknowledgments

The authors thank Conselho Nacional de Desenvolvimento Científico e Tecnológico (CNPq, Proc. 554569/210-8 and Proc. 475609/2008-5), for financial support and Coordenação de Aperfeiçoamento de Pessoal de Nível Superior (CAPES), for scholarship. Thanks are also due to Tatiane Oliveira dos Santos from Laboratório de Microscopia (LABMIC) da Universidade Federal de Goiás, Goiânia-GO, Brazil for the use of the JEOL, JEM-2010 HRTEM microscope.

References

1. Oliveira-Neto, A.; Brandalise, M.; Dias, R. R.; Ayoub, J. M. S.; Silva, A. C.; Penteado, J. C.; Linardi, M.; Spinacé, E. V.; *Int. J. Hydrogen Energ.* **2010**, *35*, 9177.
2. Spinacé, E. V.; Linardi, M.; Oliveira-Neto, A.; *Electrochem. Commun.* **2005**, *7*, 365.
3. De Souza, R. F. B.; Parreira, L. S.; Rascio, D. C.; Silva, J. C. M.; Teixeira-Neto, E.; Calegaro, M. L.; Spinace, E. V.; Oliveira-Neto, A.; Santos, M. C.; *J. Power Sources* **2009**, *195*, 1589.
4. Delime, F.; Léger, J.-M.; Lamy, C.; *J. Appl. Electrochem.* **1999**, *29*, 1249.
5. Nonaka, H.; Matsumura, Y.; *J. Electroanal. Chem.* **2002**, *520*, 101.
6. Wang, K.; Liu, C.; Chang, Y.; *Electrochim. Acta* **2011**, *562*, 574.
7. Carbonio, E. A.; Colmati, F.; Ciapina, E. G.; Pereira, M. E.; Gonzalez, E. R.; *J. Braz. Chem. Soc.* **2010**, *21*, 590.
8. Oezaslan, M.; Hasché, F.; Strasser, P.; *J. Electrochem. Soc.* **2012**, *159*, B444.
9. Huang, M.; Jiang, Y.; Jin, C.; Ren, J.; Zhou, Z.; Guan, L.; *Electrochim. Acta* **2014**, *125*, 29.
10. Lamy, C.; Rousseau, S.; Belgsir, E. M.; Counteceau, C.; Léger, J. M.; *Electrochim. Acta* **2004**, *49*, 3901.
11. Vigier, F.; Coutanceau, C.; Perrard, A.; Belgsir, E. M.; Lamy, C.; *J. Appl. Electrochem.* **2004**, *34*, 439.
12. Vigier, F.; Coutanceau, C.; Hahn, F.; Belgsir, E. M.; Lamy, C.; *J. Electroanal. Chem.* **2004**, *81*, 563.
13. Zhou, W. J.; Li, W. Z.; Song, S. Q.; Zhou, Z. H.; Jiang, L. H.; Sun, G. Q.; Xin, Q.; Poulianitis, K.; Kontou, S.; Tsiakaras, P.; *J. Power Sources* **2004**, *131*, 217.
14. Zhou, W. J. ; Song, S. Q.; Li, W. Z.; Sun, G. Q.; Xin, Q.; Kontou, S.; Poulianitis, K.; Tsiakaras, P.; *Solid State Ionics* **2004**, *175*, 797.
15. Zhou, W.; Zhou, Z.; Song, S.; Li, W.; Sun, G.; Tsiakaras, P.; Xin, Q.; *Appl. Catal., B* **2003**, *46*, 273.
16. Jiang, L.; Zhou, Z.; Li, W.; Zhou, W.; Song, S.; Li, H.; Sun, G.; Xin, Q.; *Energy Fuels* **2004**, *18*, 866.
17. Jiang, L.; Sun, G.; Zhou, Z.; Zhou, W.; Xin, Q.; *Catal. Today* **2004**, *93*, 665.
18. Zhou, W. J.; Song, S. Q.; Li, W. Z.; Sun, G. Q.; Xin, Q. S.; Kontou, K.; Tsiakaras, P.; *Solid State Ionics* **2004**, *175*, 797.
19. Colmati, F.; Antolini, E.; Gonzalez, E. R.; *Electrochim. Acta* **2005**, *50*, 5496.
20. Page, T.; Johnson, R.; Hormes, J.; Noding, S.; Rambabu, B.; *J. Electroanal. Chem.* **2000**, *485*, 34.
21. Yang, H.; Dai, L.; Xu, D.; Fang, J.; Zhou, S.; *Electrochim. Acta* **2010**, *55*, 8000.
22. Beyhan, S.; Léger, J. M.; Kadırgan, F.; *Appl. Catal., B* **2014**, *144*, 66.
23. Ribeiro, J.; dos Anjos, D. M.; Kokoh, B. K.; Coutanceau, C.; Léger, J.-M.; Olivi, P.; Andrade, A. R.; Tremiliosi-Filho, G.; *Electrochim. Acta* **2007**, *52*, 6997.
24. Silva-Junior, L. C.; Maia, G.; Passos, R. R.; Souza, E. A.; Camara, G. A.; Giz, M. J.; *Electrochim. Acta* **2013**, *112,* 612.
25. De Souza, R. F. B.; Silva, J. C. M.; Assumpção, M. H. M. T.; Oliveira-Neto, A.; Santos, M. C.; *Electrochim. Acta* **2014**, *117*, 292.
26. Silva, J. C. M.; Anea, B.; de Souza, R. F. B.; Assumpção, M. H. M. T.; Calegaro, M. L.; Oliveira-Neto, A.; Santos, M. C.; *J. Braz. Chem. Soc*. **2013**, *24,* 1553.
27. Spinacé, E. V.; Oliveira-Neto, A.; Vasconcelos, T. R. R.; Linardi, M.; *Brazilian Patent.* **2003**, (INPI-RJ, PI0304121-2).
28. Spinacé, E. V.; Oliveira-Neto, A.; Vasconcelos, T. R. R.; Linardi, M.; *J. Power Sources* **2004**, *17*, 137.
29. Ammam, M.; Easton, E. B.; *J. Power Sources* **2013**, *222*, 79.
30. Colmati, F.; Antolini, E.; Gonzalez, E. R.; *Appl. Catal., B* **2007**, *73*, 106.
31. Ammam, M.; Easton, E. B.; *J. Power Sources* **2012**, *215*, 188.
32. Colmati, F.; Antolini, E.; Gonzalez, E. R.; *J. Electrochem. Soc.* **2007**, *189*, B39.
33. Colmati, F.; Antolini, E.; Gonzalez, E. R.; *J. Alloys and Compounds* **2008**, *456*, 264.
34. Huang, T.; Lin, K.; Tung, S.; Cheng, T.; Chang, I.; Hsieh, Y.; Lee, C.; Chiu, H.; *J. Electroanal. Chem.* **2009***, 636,* 123.

35. Antolini, E.; *Int. J. Hydrogen Energ.* **2011***, 36,* 11043.
36. Mukerjee, S.; McBreen, J.; *J. Electrochem. Soc.* **1999**, *146*, 600.
37. Barroso, J.; Pierna, A. R.; Blanco, T. C.; Ruiz, N.; *Int. J. Hydrogen Energ.* **2014**, *39*, 3984.
38. Crisafulli, R.; Oliveira-Neto, A.; Linardi, M.; Spinacé, E. V.; *Stud. Surf. Sci. Catal.* **2010**, *175*, 559.
39 Zhang, S.; Yuan, X-Z.; Hin, J. N. C.; Wang, H.; Friedrich, K. A.; Schulze, M.; *J. Power Sources* **2009**, *194*, 588.

Submitted on: October 15, 2013
Published online: May 23, 2014